

# Chemical interpretation of oscillatory modes at a Hopf point

Sune Danø,<sup>\*a</sup> Mads F. Madsen<sup>b</sup> and Preben G. Sørensen<sup>b</sup>

<sup>a</sup> Department of Medical Biochemistry and Genetics, University of Copenhagen, Blegdamsvej 3b, 2200 Copenhagen N, Denmark. E-mail: [sdd@kiku.dk](mailto:sdd@kiku.dk)

<sup>b</sup> Biophysical Chemistry Group, Department of Chemistry, University of Copenhagen, Universitetsparken 5, 2100 Copenhagen Ø, Denmark

Received 5th October 2004, Accepted 21st February 2005

First published as an Advance Article on the web 11th March 2005

We present two complementary methods for studying the oscillatory mechanisms in a chemical reaction network in the neighbourhood of a supercritical Hopf bifurcation. The first method is a modification of metabolic control analysis (a form of sensitivity analysis), and focuses on the reactions rather than the chemical species. By rephrasing metabolic control analysis in terms of the amplitude equation of the Hopf bifurcation, we show that control of amplitude and frequency of the oscillations should be considered separately, and that the amplitude control is directly related to the control of the stability of the stationary state. Generally, the frequency of the oscillations is controlled by more reactions than the amplitude is, and those reactions controlling amplitude will generally also exert control of the frequency. The second method focuses on the role of the chemical species. By considering their relative phases and amplitudes, the method reveals to what extent a simple activator–inhibitor interpretation of the amplitude equation associated with the Hopf bifurcation corresponds to an equally simple chemical interpretation. If applicable, the method identifies the activating and inhibiting modes chemically. Prior knowledge of the underlying reaction network is not needed, only phase and amplitude measurements are used in the analysis. Hence, this method is a top-down approach well suited for systems biology. Both methods are exemplified by calculations on the Oregonator model for the Belousov–Zhabotinsky reaction.

## 1. Introduction

Low-dimensional activator/inhibitor models have been used extensively for the study of oscillations and patterns in biological systems.<sup>1</sup> At first sight it is surprising that such simple models can be used at all because of the high dimension of chemical state space of a biological system. The reason for this is that the observable dynamics is confined to a low-dimensional “slow” manifold embedded in the state space. This confinement is a result of the presence of fast reactions which move any state toward this “slow” manifold on a time scale which is much smaller than the time scale of observation. The “slow” dynamics is formally described by a low-dimensional set of “slow” differential equations together with an equation defining the embedding of the “slow” manifold in concentration space. The differential equations are of historic reasons called amplitude equations, and express the dynamics in a compact form using local coordinates of the “slow” manifold.

When a system operates close to a stationary state at a supercritical Hopf bifurcation, a separation of time scales as described above applies naturally. The small amplitude oscillations, which are observed in this case, are manifestations of states confined to a two dimensional “slow” manifold which contains the stationary state. On this manifold all dynamics are described by the two dimensional Stuart–Landau differential equation using two variables representing modes which can be interpreted as an activator and an inhibitor.

If a complete kinetic model is known, the connection between the mode variables and the concentrations of the chemical species can be calculated explicitly. In the next section we will, for such systems, demonstrate a universal connection between the degree of instability and the amplitude and frequency of the oscillations.

In the subsequent section we relate the simple Stuart–Landau picture to phase and amplitude data, and develop a method for determining the chemical identity of possible

activator/inhibitor modes. This method can be applied even if the kinetic mechanism for the system is unknown.

In the last section we illustrate the usefulness of the methods by applying them to the Oregonator model of the Belousov–Zhabotinsky reaction.

## 2. Sensitivity analysis at a Hopf bifurcation

### 2.1. Metabolic control analysis

Metabolic control analysis (MCA) is a variation of sensitivity analysis where the effects of infinitesimal changes of parameters are quantified. It was originally developed for studies of enzymatic networks at a stationary state, and has previously been used in the context of oscillations.<sup>2–4</sup> We shall describe a simple modification of this method that makes it applicable at a supercritical Hopf bifurcation.

The control coefficient

$$C_p^X = \frac{p}{X} \frac{\partial X}{\partial p} = \frac{\partial \ln X}{\partial \ln p} \quad (1)$$

describes the control of a parameter  $p$  on a property  $X$  (see ref. 5 for details). Here we want to discuss the control of the sinusoidal oscillations close to a Hopf bifurcation, so the natural choice of properties is frequency and amplitude of the oscillations.

A reaction rate is a linear function of a parameter  $p_r$ , if it can be written as  $v_r = p_r g(\dots x_j \dots)$  where  $x_j$  is the concentration of the  $j$ th chemical species. In this case  $p_r$  is called the velocity parameter of the reaction  $r$ . Some parameters, e.g. temperature, do not have this property. For reactions with mass action kinetics the velocity parameters are the rate constants. For enzyme reactions the velocity parameters are the maximum velocities. If this applies for all reactions, summation theorems based on time-scaling invariance can be derived. Increasing all

velocity parameters by a factor  $h$  is equivalent to rescaling the time, since this changes all the time constants of the equations by a factor of  $h^{-1}$ . This scaling leaves the trajectories in concentration space unchanged. The trajectories include stationary points and limit cycles. The summation theorems follow from eqn. (1) and

$$\frac{dX}{dh} = \sum_r \frac{\partial X}{\partial(hp_r)} \frac{\partial(hp_r)}{\partial h} \stackrel{h=1}{=} \sum_r \frac{\partial X}{\partial p_r} p_r = \sum_r X C_{p_r}^X.$$

If  $X$  is a geometric property independent of  $h$ , for example an amplitude  $A$  of a limit cycle, we have  $dX/dh = 0$  giving  $\sum_r C_{p_r}^A = 0$ . If  $X$  is a property  $\Omega$ , which scales linearly with  $h$ , such as the oscillatory frequency of a limit cycle, we have  $dX/dh = X$ , giving  $\sum_r C_{p_r}^\Omega = 1$ .

The control coefficient for the frequency of the limit-cycle oscillations  $\omega_{lc}$  is calculated in accordance with eqn. (1). The calculations for the amplitude of the limit cycle in the neighbourhood of a supercritical Hopf bifurcation need some special consideration. In the concentration space the limit cycle is an ellipse degenerating to a point at the bifurcation point. The size of the ellipse has a square root dependence on the distance from the bifurcation point. We define an amplitude as the sum of the amplitudes of each of the species  $s$ :  $a = \sum_s a_s$ ; the standard MCA definition of the control coefficient eqn. (1) will have a singularity at the bifurcation point. In order to avoid this, we have chosen instead to calculate the unscaled control coefficient of the square of the amplitude. This is given by

$$\Gamma_p^{a^2} = \frac{\partial a^2}{\partial p/p}. \quad (2)$$

By a similar argument as above we have the summation rule  $\sum_r \Gamma_p^{a^2} = 0$ .

The calculations of  $C_p^{\omega_{lc}}$  and  $\Gamma_p^{a^2}$  were performed with continuation methods using the program `cont`.<sup>6</sup> First, a continuation of the limit cycle is performed with respect to a bifurcation parameter. Subsequently, each of the data points of this continuation are used as a starting point for short-distance limit cycle continuations with each of the velocity parameters as continuation parameter. Summation theorems were used to check the validity of the calculations or, in some cases, to calculate the control coefficients of a velocity parameter which could otherwise not be calculated due to numerical difficulties. Customised scripts were used to automate the process. These scripts are available from Mads F. Madsen ([mfm@osc.kiku.dk](mailto:mfm@osc.kiku.dk)) on request.

**2.1.1. MCA at supercritical Hopf bifurcations.** The amplitude equation associated with the supercritical Hopf bifurcation is the Stuart–Landau equation

$$\dot{z} = (i\omega_0 + \sigma\mu)z + gz|z|^2 \quad (3)$$

As mentioned above, it gives a good description of the system dynamics on the slow manifold. In this equation, the local coordinate  $z = z' + iz''$  describes the state of the system,  $\sigma = \sigma' + i\sigma''$  and  $g = g' + ig''$  are complex parameters, whereas the parameters  $\mu$  and  $\omega_0$  are real. The dot denotes differentiation with respect to time. Note that in our notation the sign of  $g$  is in accordance with ref. 7, but opposite of that normally used.

It is a good approximation to replace the slow manifold with a plane spanned by the components of the complex eigenvector associated with the complex mode, which becomes unstable at the bifurcation point. We refer to the corresponding complex eigenvalue as  $\lambda$ . The frequency of oscillation at the bifurcation point is  $\omega_0$ , and  $\mu$  is a measure of the distance from the bifurcation point. The parameters  $g$  and  $\sigma$  determine the properties of the limit cycle and the rate at which stability and frequency changes with  $\mu$ , respectively. See ref. 8 for

details. The eigenvectors spanning the plane of oscillations and the parameters of eqn. (3) can be calculated from a kinetic model at a Hopf bifurcation<sup>7</sup> or estimated from experimental data.<sup>9–11</sup>

For use with MCA, we choose  $\mu = (p - p_0)/p_0$  where  $p_0$  is the value of the parameter at the bifurcation point. For each parameter  $p$  under study, this results in new values of  $\sigma'$  and  $\sigma''$  which we call  $\sigma'_p$  and  $\sigma''_p$ , whereas the values of  $\omega_0$  and  $g$  remain the same for all choices of  $p$ . The frequency and amplitude of the oscillations are

$$\omega_{lc} = \omega_0 + \left( \sigma'' - \sigma' \frac{g''}{g'} \right) \mu$$

$$a = \sqrt{\frac{-\sigma' \mu}{g'}},$$

respectively. The frequency control coefficient at the bifurcation point then becomes

$$C_p^{\omega_{lc}} = \frac{d \ln \omega}{d \ln p} = \frac{1}{\omega} \frac{d\omega}{d\mu} = \frac{1}{\omega_0} \left( \sigma''_p - \sigma'_p \frac{g''}{g'} \right). \quad (4)$$

As above (eqn. (2)), we need to avoid the singularities at the bifurcation point. Therefore, we introduce the relative rate of change of stability

$$\frac{d \operatorname{Re}(\lambda)}{dp/p_0} = \frac{d \operatorname{Re}(\lambda)}{d\mu} = \sigma'_p, \quad (5)$$

which is a scaled measure of the change of the square of the amplitude. As such, it corresponds to our definition of  $\Gamma_p^{a^2}$  (eqn. (2)). An alternative interpretation is that  $\sigma'_p$  reflects the rate of change of stability of the stationary state as the parameter in question is increased. A similar measure has previously been introduced;<sup>12</sup> the measure presented here has the advantage that the singularity at the bifurcation point is avoided.

For a given bifurcation point, we use Mathematica (Wolfram Research, Inc., Champaign, IL) to calculate sets of Stuart–Landau parameters according to the formulae given in ref. 7. Each set corresponds to choosing one of the parameters  $p$  as bifurcation parameter. Specific directions on how to perform these calculations can be obtained from Mads F. Madsen ([mfm@osc.kiku.dk](mailto:mfm@osc.kiku.dk)).

**2.1.2. MCA of stable and unstable foci.** The Stuart–Landau description is only valid close to a supercritical Hopf bifurcation. Independent of this  $\sigma'_p$  and  $\omega_0 + \mu\sigma''_p$  can be calculated for any stationary point with a complex mode as the real and imaginary part of the complex eigenvalue of the Jacobian matrix. In general they express the changes in stability and frequency, respectively, of the linear parts of this mode as some parameter  $p$  is varied. Thus, calculations of  $\sigma'_p$  and  $\sigma''_p$  can be used to characterise an oscillatory mode of a system, even when such a mode has not yet become unstable.

We first use the program `cont`<sup>6</sup> to obtain a description of the stationary state as a function of some chosen bifurcation parameter. Each of these states are evaluated for each of the parameters  $p$ . We calculate the frequency control coefficient  $C_p^{\omega_{ss}} = \sigma''_p \operatorname{Im}(\lambda)$  in agreement with standard MCA definitions (eqn. (1)), but to avoid singularities at bifurcation points we calculate  $\sigma'_p$  as an unscaled measure of the change of stability (eqn. (5)). These calculations were made with Mathematica; we exploit the fact that the Jacobian matrix  $J$  is continuous in  $\mu$ , and use a trick<sup>13</sup> from perturbation theory for linear operators to speed up the calculations. As before, a customised script was

used to automate the process. The script is available from Mads F. Madsen (mfm@osc.kiku.dk) on request.

### 3. Identification of activators and inhibitors

The methods described above allow us to analyse chemical reaction systems in terms of their reaction rates. Alternatively, one can discuss the origin of the oscillations in terms of the concentration changes of the chemical species. The simplest form of such an analysis would be to look for the species with the largest relative amplitudes, disregarding the phase information.

We will now discuss the advantages of utilising both phase and amplitude data through polar phase plane plots. We exploit the concept of universality: from the point of view of dynamics, all systems close to a supercritical Hopf bifurcation are similar. Hence, they all behave according to the simple two-dimensional Stuart–Landau equation as discussed above.

We will first show how this behaviour can be understood in terms of an activating and an inhibiting mode. These two modes form a simple orthogonal structure in the  $z$  coordinate system of the plane of oscillations. We will then show how to identify this simple structure in the chemical coordinate system. The modes of the Stuart–Landau equation and chemical species are not necessarily equivalent, and it might not be possible to identify the Stuart–Landau modes in terms of chemical species or simple combinations thereof. However, if it is possible to identify two chemical modes which correspond to the two Stuart–Landau modes, then we can use the simple understanding in terms of dynamics to obtain an equally simple understanding of the oscillations in terms of chemistry.

We start by writing the real and imaginary parts of the Stuart–Landau equation (eqn. (3)) explicitly

$$\begin{aligned} z' &= \mu\sigma'z' - (\omega_0 + \mu\sigma'')z'' + g'z'(z'^2 + z''^2) - g''z''(z'^2 + z''^2) \\ z'' &= \mu\sigma'z'' + (\omega_0 + \mu\sigma'')z' + g'z''(z'^2 + z''^2) + g''z'(z'^2 + z''^2), \end{aligned}$$

and from this we calculate the Jacobian matrix (see, e.g. refs. 8 and 14) at the stationary state  $z = 0$

$$\mathbf{J}|_{z=0} = \begin{bmatrix} \mu\sigma' & -(\omega_0 + \mu\sigma'') \\ \omega_0 + \mu\sigma'' & \mu\sigma' \end{bmatrix}. \quad (6)$$

After the onset of the oscillations, the signs of the elements of  $\mathbf{J}$  are

$$\begin{bmatrix} + & - \\ + & + \end{bmatrix}.$$

The linearised dynamics in the plane of oscillations is composed of the two Stuart–Landau modes  $z'$  and  $z''$ . Above the bifurcation point (i.e. for  $\mu\sigma' > 0$ ), both of these Stuart–Landau modes are autocatalytic, and the strength of the autocatalysis is given by  $\mu\sigma'$  (positive diagonal terms of the Jacobian). The tendency to oscillate is due to the asymmetry in the two off-diagonal terms  $\pm(\omega_0 + \mu\sigma'')$ . The + in the lower left corner indicates that the  $z'$  mode is an activator of the mode  $z''$ , whereas the negative element indicates that the  $z''$  mode is an inhibitor of the  $z'$  mode. It follows that these two modes are separated by  $90^\circ$  in the  $z$  coordinate system.

We will now address the question of how to identify the two Stuart–Landau modes chemically. In chemical concentration space, they correspond to two directions in the plane of oscillations. However, these directions will generally not be separated by  $90^\circ$  in this space.

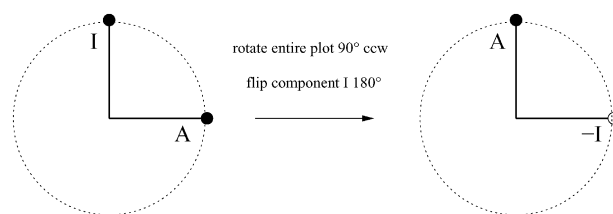
We use polar phase plane plots to visualise the chemical plane of oscillations. They reflect the relative positions of the different chemical species in the  $z$ -coordinate system of the complex (oscillatory) eigenmode. Hence the advantage of these plots is that the  $90^\circ$  structure of the Stuart–Landau modes is retained. The plots are constructed so that the angles are the relative phases  $\theta_s$  of the chemical species, and the distances from the centre is given by their relative amplitudes  $a_s$ . The

relative phases and amplitudes are either measured or calculated from the complex eigenvector  $\mathbf{u}$  of the plane of oscillation. The component of species  $s$  of this eigenvector is given by  $u_s = a_s \exp(i\theta_s)$ . (In order to comply with the usual convention for relative phases, one must choose  $\mathbf{u}$  as the eigenvector corresponding to the eigenvalue  $-\omega$  at the bifurcation point.) These calculations were made with Mathematica.

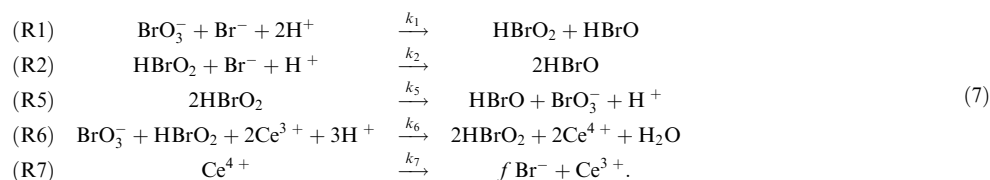
The identification of the Stuart–Landau modes in chemical terms is complicated by the fact that  $\mathbf{u}$  is not uniquely defined, since any complex vector  $\hat{\mathbf{u}} = \alpha\mathbf{u}$  obtained by multiplying a complex eigenvector  $\mathbf{u}$  by a non-zero complex number  $\alpha$  is itself an eigenvector associated with the same eigenvalue. It follows that by choosing  $\alpha$  we can scale modulus of all components of the complex eigenvector and shift their phases. Accordingly, only the relative amplitudes and the relative phases contain information about the dynamics of the system.

When seeking a chemical interpretation of the Stuart–Landau modes, we must therefore rotate the chemical polar phase plane plot looking for maximal projections of the chemical components onto the Stuart–Landau modes which, by convention, are found at  $0^\circ$  and  $90^\circ$ . If we find such chemical modes with large components from a few species, then we conclude that these species are essential, and we know what the roles of these species are in the oscillations. This knowledge can then be used to devise an explanation of the mechanism of oscillations in chemical terms. If, on the other hand, the  $90^\circ$  structure of the Stuart–Landau modes is not reflected in a chemical structure of approximately  $90^\circ$ , then we conclude that the Stuart–Landau modes are composed of many species without any of them being dominating, or that many species play dual roles in the underlying dynamics.

To ease the interpretation, it is sometimes an advantage to flip the phase of some chemical species  $180^\circ$ , and then think of this component as scarcity of the species in question. That is, we plot the relative phase of the minimum of this particular species instead of that of its maximum. As we will now show, this does not affect the chemical conclusions. The polar phase plane plot in the left part of Fig. 1 indicates that abundance of component A is the activating mode and abundance of component I is the inhibiting mode. The chemical conclusion drawn from this is  $\partial[\text{I}]/\partial[\text{A}] > 0$  and  $\partial[\text{A}]/\partial[\text{I}] < 0$  (eqn. (6)). We then flip component I and rotate the entire plot to realign with the  $0^\circ$  and  $90^\circ$  directions. The activating mode now becomes scarcity of component I, and the inhibiting mode becomes abundance of component A (right part of Fig. 1). The chemical conclusions read from this plot are  $\partial[\text{A}]/\partial(-[\text{I}]) > 0$  and  $\partial(-[\text{I}])/\partial[\text{A}] < 0$ , which are equivalent to those of the first plot. One can easily show that all permutations lead to the same chemical conclusions. Since more than one interpretation is possible, the important point is not simply to name “the



**Fig. 1** Schematic polar phase plane plots illustrating that “flipping” does not alter the chemical conclusions. The plot on the left indicates the  $90^\circ$  phase delay between an activating component A and an inhibiting component I. The corresponding chemical conclusions are  $\partial[\text{I}]/\partial[\text{A}] > 0$  and  $\partial[\text{A}]/\partial[\text{I}] < 0$  (eqn. (6)). In the right part of the figure, we plot scarcity of component I instead of abundance of component I, and then rotate the entire plot to realign with the  $0^\circ$  and  $90^\circ$  directions. The activating mode is now scarcity of component I, and the inhibiting mode is abundance of component A. In agreement with the plot on the left, the chemical conclusions for the plot on the right are  $\partial[\text{A}]/\partial(-[\text{I}]) > 0$  and  $\partial(-[\text{I}])/\partial[\text{A}] < 0$ . Abundance is indicated by ● and scarcity is indicated by ○ in the plots. ccw: counterclockwise.

**Table 1** Chemical reactions of this version of the Oregonator model

activator” and “the inhibitor”. Instead, the key point is that the chemical basis for the possible interpretations are the same.

The “flipping” helps to make chemical structures of approximately  $90^\circ$  more clear, and some double negations can be avoided in the interpretation. The procedure is exemplified in the next section.

Our approach can be understood in terms of the real and imaginary parts of the complex eigenvector  $\mathbf{u} = \mathbf{v} + i\mathbf{w}$ . The rotation of the polar phase plane plot is a graphical procedure for finding the maximal elements of these vectors. The “flipping” means that we look for elements of maximal magnitude, irrespective of sign.

#### 4. Results for the Oregonator model

In this section, we exemplify the calculations of control coefficients and the use of polar phase plane plots with the Oregonator model<sup>15</sup> describing the thoroughly studied oscillations of the Belousov–Zhabotinsky reaction system (see *e.g.* ref. 16) in a continuous-flow stirred tank reactor (CSTR). For notation, operating point and parameter values we shall refer to ref. 17.

The chemical reactions of this version of the Oregonator model are listed in Table 1. The rate equations are derived from reactions (7) assuming mass-action kinetics. The dynamic variables are  $[\text{HBrO}_2]$ ,  $[\text{Br}^-]$ , and  $[\text{Ce}^{4+}]$ .  $[\text{BrO}_3^-]$ ,  $[\text{H}^+]$  and  $[\text{H}_2\text{O}]$  are considered constant.  $[\text{HBrO}]$  does not enter the rate equations, and  $[\text{Ce}^{3+}]$  only enters the rate equations *via* the stoichiometric constraint  $[\text{Ce}^{3+}] + [\text{Ce}^{4+}] = [\text{Ce}^{3+}]_0$ . To account for the specific flow of the CSTR, an outflow term of the form  $-k_0[\text{X}]$  is added for each of the three variables. The feed species of the CSTR are  $\text{BrO}_3^-$  and  $\text{Ce}^{3+}$ . The inflow enters the rate equations through the mixed flow concentrations  $[\text{Ce}^{3+}]_0$  and  $[\text{BrO}_3^-]_0$ .

Reaction (R7) (with the empirical stoichiometric factor  $f$ ) is a schematic reaction summarising the complicated organic subset of the Belousov–Zhabotinsky reaction system: oxidation of malonic acid drives the reaction system *via* reduction of  $\text{Ce}^{4+}$ , and bromide is produced in the process.

Reaction (R6) of the Oregonator is autocatalytic in  $\text{HBrO}_2$ ; this is considered the source of the instability of the stationary point. Reaction (R6) produces  $\text{Ce}^{4+}$  as well as  $\text{HBrO}_2$ , and subsequently reaction (R7) generates  $\text{Br}^-$  from  $\text{Ce}^{4+}$ . The specific flow  $k_0$  is used as bifurcation parameter. The system

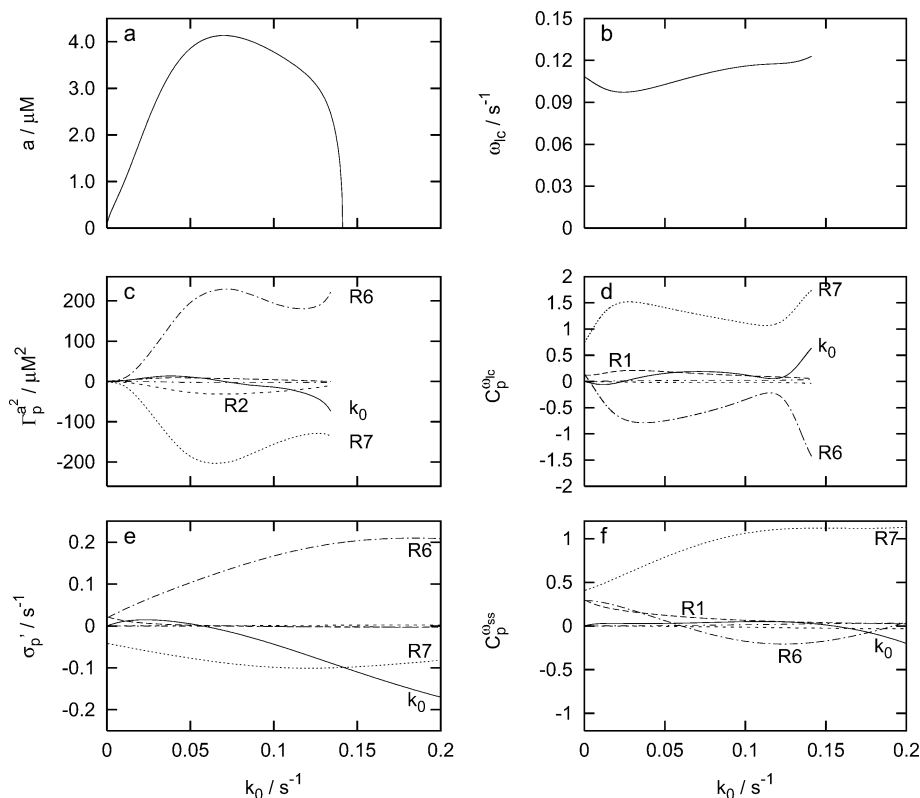


**Fig. 2** Amplitude, frequency and sensitivity analysis of the Oregonator model at various operating points. The bifurcation parameter is the specific flow rate of the CSTR,  $k_0$ . a: amplitude of the oscillations  $a = \sum_s a_s$ . b: frequency of the oscillations. c: unscaled control coefficients for the squared amplitude  $\Gamma_p^2$  (eqn. (2)). d: control coefficients  $C_p^{\text{osc}}$ , for the frequency of oscillations on the limit cycle. e: calculations of the relative rates of change of stability in the stationary state (eqn. (5)). f: control coefficients for the frequency in the stationary state. (For graphical reasons, not all lines have been annotated in panels c–f. The same line coding is used in these four panels, and the remaining annotations can be deduced by comparison.)

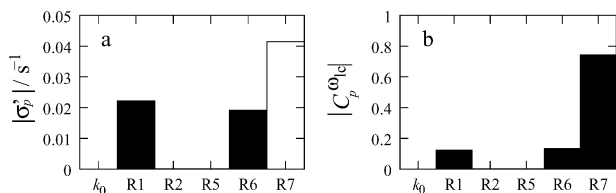


**Fig. 3** Stuart-Landau based MCA at the supercritical Hopf bifurcation found at  $k_0 = 2.99 \times 10^{-5} \text{ s}^{-1}$ . a: relative rate of change of stability for the rate constants of the Oregonator (corresponds to the left-most parts of Fig. 2c and 2e). b: frequency control coefficients (corresponds to the left-most part of Fig. 2d). Black bars represent positive coefficients and white bars negative coefficients.

has supercritical Hopf bifurcations at  $k_0 = 2.99 \times 10^{-5} \text{ s}^{-1}$  and at  $k_0 = 0.141 \text{ s}^{-1}$  (Fig. 2a and 2b).

#### 4.1 MCA of limit-cycle oscillations

Fig. 2c and 2d show an example of limit-cycle MCA calculations for the Oregonator. The bifurcation parameter is the specific flow rate of the reactor, and the plots span the entire range of oscillations. In the thermodynamic limit on the left, the flow rate is very low, and the oscillations disappear because the system comes too close to equilibrium. In the convective limit on the right, the specific flow is so high that the oscillations disappear because there is too little time for the chemical species to react (washout). In the limit-cycle MCA, this is reflected by  $\Gamma_{k_0}^{\omega}$  which is positive at low flow rates, but becomes negative and of large magnitude at high flow rates. The autocatalytic reaction (R6) has by far the largest positive  $\Gamma_p^{\omega}$  coefficient; this agrees with the chemical expectations as indicated above. Likewise, the bromide-forming reaction (R7) has the largest negative  $\Gamma_p^{\omega}$  coefficient. For intermediate flow rates, the stabilisation of the limit cycle by reaction (R2) is seen. Reactions (R6) and (R7) also have the largest shares of the frequency control, whereas reaction (R1) and  $k_0$  have a smaller fraction of control.

#### 4.2 Stuart-Landau based MCA

The  $C_p^{\omega}$  and  $\sigma_p'$  coefficients at the supercritical Hopf bifurcation at  $k_0 = 2.99 \times 10^{-5} \text{ s}^{-1}$  are shown in Fig. 3a and 3b. The interpretation agrees with that of the limit-cycle continuation (Fig. 2c and 2d): reactions (R1), (R6) and (R7) dominate, and Fig. 3a shows that the  $\text{HBrO}_2$ -producing reactions (R1) and (R6) tend to make the stationary state unstable, whereas the  $\text{Br}^-$ -forming reaction (R7) stabilises the stationary state. Fig. 3b shows that all reactions increase the frequency of oscillations, and that reaction (R7) has the largest control of frequency.

#### 4.3 MCA of stable and unstable foci

Fig. 2e and 2f show calculations of  $\sigma_p'$  and  $\sigma_p''$  as functions of  $k_0$ . These coefficients reflect the control exerted by the various reactions on the stability and the frequency, respectively, of oscillations close to the stationary state. It is seen that these results give the same overall picture as those obtained by MCA of the limit cycle (Fig. 2c and 2d), but some differences are found. These differences reflect the differences between the dynamics of the unstable stationary state and of the limit cycle.

#### 4.4 Polar phase plane plot analysis

Fig. 4a shows a polar phase plane plot for the Oregonator at the supercritical Hopf bifurcation found at  $k_0 = 2.99 \times 10^{-5} \text{ s}^{-1}$ . An almost  $90^\circ$  structure with  $\text{Ce}^{4+}$  close to  $0^\circ$  and  $\text{Br}^-$  at approximately  $90^\circ$  is evident. The activating mode is mainly  $\text{Ce}^{4+}$ , and the inhibiting mode is mainly  $\text{Br}^-$ . The activator

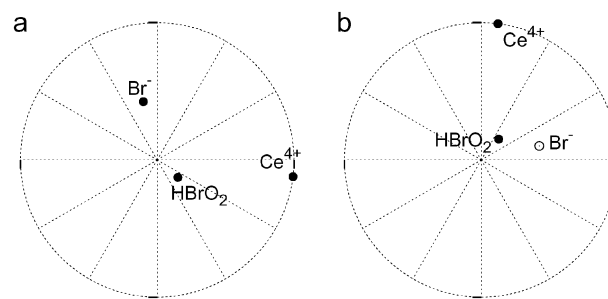


**Fig. 4** Polar phase plane plots for the Oregonator at the Hopf bifurcation at  $k_0 = 2.99 \times 10^{-5} \text{ s}^{-1}$ . Panel a shows the relative phases and amplitudes of the chemical species rotated such that the activator is  $\text{Ce}^{4+}$  and the inhibitor is  $\text{Br}^-$ . Panel b shows another possible interpretation, where the activator is "scarcity of  $\text{Br}^-$ " (indicated by  $\circ$  instead of  $\bullet$ ), and the inhibitor is  $\text{Ce}^{4+}$ . (Panel b is constructed from panel a by  $90^\circ$  counterclockwise rotation of all species followed by  $180^\circ$  flipping of  $\text{Br}^-$ ) See text for discussion.

$\text{Ce}^{4+}$  activates the inhibitor  $\text{Br}^-$  via reaction (R7). The inhibition can be understood as the removal of  $\text{HBrO}_2$  through reaction (R2) which results in less  $\text{Ce}^{4+}$  production through R6.

$\text{HBrO}_2$  has substantial components in both the activating and the inhibiting modes. This can be understood in terms of its participation in both  $\text{Br}^-$  removing and producing reactions (reaction (R2) and the combined effect of reactions (R6) and (R7), respectively). This is characteristic for the Hopf point of the thermodynamic limit; in the convective limit, the components of  $\text{HBrO}_2$  are almost exclusively in the activating (*i.e.*  $\text{Ce}^{4+}$ ) mode.

As discussed in section 3, alternative phase plane plots are possible. For example, one could flip  $\text{Br}^-$   $180^\circ$  turning it into "scarcity of bromide" and then rotate the entire plot  $90^\circ$  counterclockwise (Fig. 4b). In this interpretation, the activator mode would consist of "scarcity of bromide", and the inhibitor of this mode would be  $\text{Ce}^{4+}$ . We see that the chemical basis for this interpretation is the same as for the above:  $\text{Ce}^{4+}$  inhibits the formation of "scarcity of  $\text{Br}^-$ " through reaction (R7), and "scarcity of  $\text{Br}^-$ " increases the  $\text{Ce}^{4+}$  concentration through reactions (R2) and (R6).

This analysis is in agreement with our previous discussions of the Oregonator. Note, however, that the polar phase plane plot analysis does not reveal the autocatalytic properties of  $\text{HBrO}_2$  because of its dual role in the thermodynamic limit. A related phenomenon is seen in the sensitivity analysis (Fig. 2c–f), where the importance of reaction (R6), which is autocatalytic in  $\text{HBrO}_2$ , becomes much more pronounced as  $k_0$  is increased above the Hopf bifurcation in the thermodynamic limit.

## 5. Discussion

In this work we have devised two novel approaches to the identification of oscillatory mechanisms in chemical reaction systems. Both approaches are based on the amplitude equation of the supercritical Hopf bifurcation, and as such they are only applicable close to a Hopf point. Most oscillatory systems can, however, be pushed to a Hopf point by changing parameter values, although there is no guarantee that the Hopf point is physically realisable.

The polar phase plane plot approach is an entirely new method that relates the universal modes of the amplitude equation to sets of chemical species. The other approach is an extension of existing methods, that allow metabolic control analysis to be applied to oscillatory systems.<sup>2–4</sup> A general approach to the identification of oscillatory mechanisms has previously been discussed by Eiswirth and coworkers<sup>18</sup> (see also ref. 19). Their approach does not depend on the presence

of a Hopf bifurcation, but instead on knowledge of the full reaction mechanism, which is often not available.

We have illustrated the methods on a simple Oregonator model for the Belousov–Zhabotinsky reaction, where the oscillatory mechanism is already well established. The results from our methods are in mutual agreement, and also in agreement with the established understanding of the Oregonator model.

A particular advantage of the polar phase plane plot analysis is that it can be performed without detailed knowledge of the structure of the reaction network. If one can show that an experimental system is close to a supercritical Hopf bifurcation, then the only data needed is measurements of the relative phases and amplitudes of the relevant chemical species. It is of course important to include all relevant species in this analysis. Data sets which are essentially complete are becoming increasingly available with the use of high-throughput methods in transcriptomics, proteomics and metabolomics. At the same time, the move towards systems biology has the effect that the complexity of the systems under study is increasing dramatically, and, consequently, it is difficult to assure a detailed understanding of the reaction network. Based on such considerations, we suggest that analysis by means of polar phase plane plots will become a valuable top-down approach for systems biology. A related study<sup>20</sup> serves as proof of concept for this idea. We have previously shown that yeast cells exhibiting glycolytic oscillations are close to a supercritical Hopf bifurcation,<sup>21,11</sup> and in our recent work<sup>20</sup> we use polar phase plane plots constructed from experimental data to settle the long-standing debate of the mechanisms responsible for glycolytic oscillations in yeast cells.

The two Stuart–Landau modes govern the behaviour of any system close to a supercritical Hopf bifurcation. It is, however, an open question whether the separation of the chemical species in two corresponding groups is possible in general. Our analysis of glycolysis shows, that it is possible in this particular case.

Combining MCA with the amplitude equation of the supercritical Hopf bifurcation has given a more precise understanding of MCA results for oscillatory systems. We have shown an explicit link between control of amplitude and control of stability of the stationary state. The frequency of oscillation is generally influenced by larger parts of the reaction network than those influencing the stability. This is seen from eqns. (4) and (5): frequency control is the sum of the  $\sigma'_p$  and the  $\sigma''_p$  contributions, whereas control of stability is determined by  $\sigma'_p$  only. Consequently, one should discuss the control of frequency and the control of stability separately, but remember that those components controlling stability will generally also control frequency, whereas the opposite is not the case. Due to the small size of the reaction network, this is not seen in the case of the Oregonator, but the effect is clearly seen in the case of glycolytic oscillations.<sup>20</sup> This result is surprising when seen in the context of MCA, where one would usually argue in terms

of the summation laws derived from time scaling. Since amplitude control sums to zero, no single reaction can have full control of amplitude, but a single reaction can, in principle, have full control of frequency, since the frequency control coefficients sum to one. A bold, but nevertheless accepted, extrapolation of this argument leads to the erroneous conclusion that amplitude control tends to be distributed among more reactions than frequency control.

## Acknowledgements

This work has been supported by the Functional Dynamics initiative of the Danish Natural Science Research Council. S. D. acknowledges the financial support provided by the Villum Kann Rasmussen Foundation, and we all acknowledge the EU-Commission, BioSim, Contract no. 005137.

## References

- 1 H. Meinhardt, *The Algorithmic Beauty of Sea Shells*, Springer Verlag, Berlin, 1995.
- 2 M. Bier, B. Teusink, B. N. Kholodenko and H. V. Westerhoff, *Biophys. Chem.*, 1996, **62**, 15–24.
- 3 B. Teusink, B. M. Bakker and H. V. Westerhoff, *Biochim. Biophys. Acta*, 1996, **1275**, 204–212.
- 4 K. A. Reijenga, H. V. Westerhoff, B. N. Kholodenko and J. L. Snoep, *Biophys. J.*, 2002, **82**, 99–108.
- 5 D. Fell, *Understanding the Control of Metabolism*, Portland Press, London, 1997.
- 6 M. Kohout, I. Schreiber and M. Kubiček, *Comput. Chem. Eng.*, 2002, **26**, 517–527.
- 7 M. Ipsen, F. Hynne and P. G. Sørensen, *Chaos*, 1998, **8**, 834–852.
- 8 Y. Kuramoto, *Chemical Oscillations, Waves, and Turbulence*, Springer Verlag, Berlin, 1984.
- 9 J. Kosek, P. G. Sørensen, M. Marek and F. Hynne, *J. Phys. Chem. A*, 1994, **98**, 6128–6135.
- 10 E. Mihaliuk, H. Skødt, F. Hynne, P. G. Sørensen and K. Showalter, *J. Phys. Chem.*, 1999, **103**, 8246–8251.
- 11 F. Hynne, S. Danø and P. G. Sørensen, *Biophys. Chem.*, 2001, **94**, 121–163.
- 12 K. A. Reijenga, *Dynamic Control of Yeast Glycolysis*, PhD Thesis, Vrije Universiteit Amsterdam, 2002.
- 13 T. Kato, *Perturbation Theory for Linear Operators*, Springer-Verlag, Berlin, 1966, p. 75.
- 14 S. H. Strogatz, *Nonlinear Dynamics and Chaos*, Addison Wesley, Reading, MA, 1994.
- 15 R. J. Field and R. M. Noyes, *J. Chem. Phys.*, 1974, **60**, 1877–84.
- 16 S. K. Scott, *Chemical Chaos*, Oxford University Press, Oxford, 1993.
- 17 K. Nielsen, F. Hynne and P. G. Sørensen, *J. Chem. Phys.*, 1991, **94**, 1020–1029.
- 18 M. Eiswirth, A. Freund and J. Ross, *Adv. Chem. Phys.*, 1991, **80**, 127–199.
- 19 B. Goldstein, G. Ermakov, J. J. Centelles, H. V. Westerhoff and M. Cascante, *Eur. J. Biochem.*, 2004, **271**, 3877–3887.
- 20 M. F. Madsen, S. Danø and P. G. Sørensen, *FEBS J.*, 2005, in press.
- 21 S. Danø, P. G. Sørensen and F. Hynne, *Nature*, 1999, **402**, 320–322.